

Polyurethanes containing platinum in the main chain: Synthesis, structure and mechanofluorochromism

Hiromitsu Sogawa^{a*}, Momoka Abe^a, Ryuhei Shintani^a, Taichi Sotani^a, Kazuki Tabaru^a, Takeshi Watanabe^b, Yasushi Obora^a, Fumio Sanda^{a*}

^a*Department of Chemistry and Materials Engineering, Faculty of Chemistry, Materials and Bioengineering, Kansai University, 3-3-35 Yamate-cho, Suita, Osaka 564-8680, Japan.*

^b*Japan Synchrotron Radiation Research Institute (JASRI), 1-1-1, Kouto, Sayo-cho, Sayo-gun, Hyogo 679-5198, Japan*

*Corresponding Authors. E-mail: sogawa@kansai-u.ac.jp, sanda@kansai-u.ac.jp.

Keywords

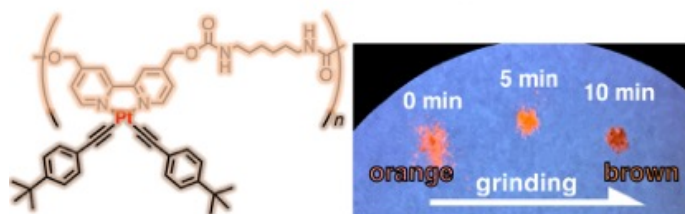
Elastomer; Mechanochromism; Mechanofluorochromism; Metallopolymer; Platinum; Polyurethane

Running Head

Mechanofluorochromic platinum-containing polyurethanes

Graphical abstract

Mechanofluorochromic Pt-containing polyurethanes



Abstract

Hydroxy-tethered platinum(II) complexes were synthesized and used as diol monomers for polyurethane synthesis. Polyurethanes with moderate molecular weights were obtained by the conventional polyaddition with a diisocyanate. The polyurethane containing platinum(II) complex substituted with *t*-Bu groups was well soluble in common organic solvents including CHCl₃ and tetrahydrofuran. Segmented polyurethanes containing platinum(II) complex moieties were also synthesized using polytetrahydrofuran and 1,4-butanediol. They showed good elastic properties. The non-segmented polyurethane exhibited distinguishable photoluminescence changes upon grinding in the solid state, while the segmented polyurethanes did not.

Introduction

Mechanochromic and mechanofluorochromic polymers are one of smart stimuli-responsive materials, whose appearance and photoluminescent colors can be tuned by mechanical force [1-5]. These polymers are applicable to stress-sensing materials and evaluation of fracture mechanism. Various mechano(fluoro)chromic polymers containing mechanophores in their main chains have been developed, in which the applied mechanical force is transferred along the polymer chains and also mechanophores, resulting in mechano(fluoro)chromism. Sottos and coworkers discovered force-induced color changes of spiropyran-containing polymethacrylates as a pioneering work [6,7]. Otsuka and coworkers developed a series of diarylbibenzofuranone-containing mechanochromic polymers [8-12]. With use of polyurethanes (PUs) and vinyl polymers as the main chain scaffolds, colored stable radicals were generated by applying mechanical force in the air. Sagara, Weder and coworkers reported mechanically responsive luminescent PUs containing cyclophane mechanophores. The applied force induced conformational changes of pyrene-containing cyclophane units, leading to content changes between monomer and excimer emission [13]. They also reported perylene-diimide-containing mechanofluorochromic polymers that change photoluminescent color based on the same principle [14].

Several organometallic compounds display photoluminescence color changes in response to mechanical force [15-17]. Ito and coworkers developed mechanofluorochromic crystals of gold

(Au) complexes [18-20]. The photoluminescence color was changed by aurophilic interaction caused by proximity distance between the Au atoms in the crystalline state. In other words, tuning of metal-metal electronic interaction is a key for exhibiting mechano(fluoro)chromism. Some platinum (Pt) complexes exhibit similar mechanoresponsive photoluminescent changes. A series of Pt(II) complexes have been reported so far, in which coordinated with NCN and NNN pincer-type ligands [21-25], 2,2'-bipyridine ligands [26-29] and others [30-32]. In spite of these numerous efforts, the combination of mechano(fluoro)chromic Pt complexes and polymeric materials is quite limited. Li *et al.* reported that Nafion embedded with Pt(II) complexes served as singlet oxygen photosensitizers but the detailed mechanisms of optical properties and mechano(fluoro)chromism were unclear [33,34]. He, Bu and coworkers end-functionalized poly(ethylene oxide)-*block*-polystyrenes with a Pt(II) complex to find luminescence changes by self-assembling into micelle and lamellar microstructures [35]. Nevertheless, no mechanofluorochromism was discussed in this work. Rowan and coworkers successfully fabricated vapochromic and mechanochromic films by blending a cationic Pt(II) complex and an NNN pincer ligand with a polymethacrylate matrix [36]. This result is very fascinating due to easy preparation, but bleaching of Pt complexes likely becomes an issue in practical applications. We synthesized a variety of Pt-containing polymers focusing on the control of higher-order structures and photoluminescent properties. The formed polymers exhibited stimuli-response of higher-order structures [37-46], catalysis [47] and triplet-

triplet annihilation photon upconversion [48,49]. Based on these backgrounds, we came up with an idea that mechanofluorochromic Pt-containing polymers, which are exempt from bleaching of Pt complexes, may be fabricated by incorporating mechanofluorochromic Pt complex moieties into a PU main chain as a scaffold, because PU is widely utilized as engineering materials featuring good processability, moldability and recyclability [50-52]. In the present study, we synthesized Pt-containing PUs using a Pt(II) complex ligated with 4,4'-bis(hydroxymethyl)-2,2'-bipyridine [bpy(CH₂OH)₂] (**1**) as a diol monomer. We examined the polyaddition of **1** and 1,6-hexamethylene diisocyanate (**2**) to obtain Pt-containing PUs, and evaluated their mechano(fluoro)chromism.

EXPERIMENTAL

Materials

All solvents for the reaction were desiccated by molecular sieve 4A and degassed by Ar bubbling before use. 2,2'-Bipyridine-4,4'-dimethanol [Bpy(CH₂OH)₂], CuI, hexamethylene diisocyanate (**2**), dibutyltin dilaurate (DBTDL), and 1,4-butanediol (BDO) were purchased from Tokyo Chemical Industry Inc. (Tokyo, Japan). Polytetrahydrofuran (PTHF, $M_n = 2000$) and K₂PtCl₄ were purchased from FUJIFILM Wako Pure Chemical Corporation (Osaka, Japan). *p-t*-Butylphenylacetylene and phenylacetylene were purchased from Sigma-Aldrich (St. Louis, USA). All other reagents were commercially obtained and used as received without purification.

Instruments

¹H (400 MHz) nuclear magnetic resonance (NMR) spectra were recorded on a JEOL JNM-ECZ400 and a JEOL JNM-ECS400 spectrometers. Infrared (IR) spectra were measured on a JASCO FT/IR-4100 spectrophotometer. For attenuated total reflection (ATR) measurements, ATR PRO410-S equipped with a Ge prism was used. Mass spectra were measured on a Bruker Compact QToF mass spectrometer using an electrospray ionization (ESI) probe under the following conditions: solvent, acetone/*i*-PrOH; mass range (m/z) < 2000; mode, negative. Peak-top molecular weight (M_p), weight-average molecular weight (M_w) and dispersity (D) values of polymers were

determined by size exclusion chromatography (SEC) on a JASCO SEC system consisting of (i) RI-930, UV-4570, PU-4580, DG-2080-53, CO-965, LC-NetII/ADC, equipped with Shodex TSK gel α -M and GMHXL, using a solution of LiBr (10 mM) in *N,N*-dimethylformamide (DMF) as an eluent at a flow rate of 1.0 mL/min, calibrated by polystyrene standards at 40 °C, and (ii) JASCO RI-4030, UV-4075, PU-4180, CO-4060, LC-NetII/ADC and AS-2055 Plus, equipped with Shodex LF-804, using tetrahydrofuran (THF) as an eluent at a flow rate of 1.0 mL/min, calibrated by polystyrene standards at 40 °C. UV–vis absorption spectra were recorded in a quartz cell (optical path length: 1 cm) on a SHIMADZU UV-2600 spectrophotometer. UV–vis diffuse reflectance spectra were recorded on a SHIMADZU UV-2600 spectrophotometer. Photoluminescence spectra were recorded in a quartz cell (optical path length: 1cm) on a SHIMADZU spectrofluorophotometer RF-6000. Mechanical properties were evaluated using a SHIMADZU EZ–Test, SMT–500N lap shear test machine at an elongation rate of 50 mm/min. Samples for the tensile test were fabricated using a punching blade conformed to ISO 37-4 specimens (dumbbell shape, 12 mm \times 2 mm) from film samples. The measurements were conducted over three times for each condition to ensure reproducibility. Small-angle X-ray scattering (SAXS) measurements were performed at BL19B2 in SPring-8 [53]. The scattered profile from the sample was collected using an area detector (PILATUS 2M). The distance between the sample and detector was 2040 mm, which was calibrated by observing the diffraction patterns of standard silver-behenate powders.

The integration time for each profile was 100 s. The obtained two-dimensional SAXS patterns were occasionally converted to a one-dimensional profile by conducting the circular average.

Synthesis of [bpy(CH₂OH)₂]PtCl₂

Bpy(CH₂OH)₂ (1.08 g, 5.00 mmol) and K₂PtCl₄ (2.07 g, 5.00 mmol) were dissolved in a mixture of THF (4 mL) and 1.0 M HCl aq. (5.67 mL) under Ar, and the resulting mixture was refluxed at 80 °C for 12 h. Then, THF (25 mL) and H₂O (25 mL) were added to the mixture, and the resulting mixture was further stirred at room temperature for 1 h to afford a solvent-insoluble residue. It was separated by filtration using a membrane (ADVANTEC H020A047A), and dried *in vacuo* to obtain [bpy(CH₂OH)₂]PtCl₂ (2.28 g, 4.73 mmol) as a yellow solid in 95% yield. ¹H NMR (400 MHz, DMSO-*d*₆): δ 9.33 (d, *J* = 6.3 Hz, 2H), 8.39 (s, 2H), 7.73 (d, *J* = 5.9 Hz, 2H), 5.89–5.77 (m, 2H), 4.79–4.64 (m, 4H) ppm. IR (KBr): 3445, 3068, 2901, 1990, 1731, 1620, 1427, 1059 cm⁻¹.

Synthesis of 1a

[Bpy(CH₂OH)₂]PtCl₂ (723 mg, 1.50 mmol) and CuI (28.6 mg, 0.15 mmol) were dissolved in a mixture of *N*-methyl-2-pyrrolidone (NMP, 8 mL) and Et₃N (3 mL) under Ar. Then, phenylacetylene (0.70 mL, 6.00 mmol) was added to the mixture, and the resulting mixture was stirred at 60 °C for overnight. After cooling to room temperature, MeOH (250 mL) was added to the mixture, stirred

for 30 min, and stored at 0 °C for 30 min. A solvent-insoluble residue was filtrated using a membrane (ADVANTEC H020A047A) and dried *in vacuo* to obtain **1a** (451 mg, 0.73 mmol) as a yellow solid in 49% yield. ¹H NMR (400 MHz, DMSO-*d*₆): δ 9.42–9.19 (m, 2H), 8.54–8.40 (m, 2H), 7.85–7.70 (m, 2H), 7.45–7.12 (m, 10H), 5.79 (s, 2H), 4.78–4.64 (m, 4H) ppm. ¹³C NMR (100 MHz, DMSO-*d*₆): δ 61.9, 121.0, 125.8, 128.5, 131.8, 150.1, 155.8, 156.8 ppm. IR (KBr): 3411, 3071, 2899, 2120, 2109, 1657, 1620, 1592, 1486, 1030 cm⁻¹. ESI-MS (m/z): calcd. 648.1462 ([C₂₈H₂₂N₂O₂Pt + 2H₂O – H]⁻), found 648.1087.

Synthesis of **1b**

Compound **1b** was synthesized in a manner similar to **1a** using *p-t*-butylphenylacetylene instead of phenylacetylene. Yield 74%. ¹H NMR (400 MHz, DMSO-*d*₆): δ 9.45–9.40 (m, 2H), 8.48 (s, 2H), 7.77 (d, *J* = 5.9 Hz, 2H), 7.28–7.23 (m, 8H), 5.79 (t, *J* = 5.4 Hz, 2H), 4.70–4.66 (m, 4H), 1.24 (d, *J* = 6.3 Hz, 18H) ppm. ¹³C NMR (100 MHz, DMSO-*d*₆): δ 31.6, 37.4, 60.9, 120.8, 125.4, 131.4, 148.3, 156.0, 157.2 ppm. IR (KBr): 3433, 3030, 2961, 2867, 2113, 1620, 1557, 1501, 1425, 1394, 1363, 1268 cm⁻¹. ESI-MS (m/z): calcd. 760.2714 ([C₃₆H₃₈N₂O₂Pt + 2H₂O – H]⁻), found 760.2282.

Synthesis of Pt-containing PUs

Typical procedure is as follows. Compound **1a** (61.3 mg, 0.100 mmol) was dissolved in NMP (1

mL) under Ar. Compound **2** (16.0 μL , 0.100 mmol) and DBTDL (1.80 μL , 3.0 μmol) were added to the solution, and the resulting mixture was stirred at 60 °C for 6 h. A yellowish solid precipitated during the reaction. MeOH (0.20 mL) was added to the mixture, and the resulting mixture was stirred for 30 minutes at room temperature to quench the reaction. MeOH (15 mL) was further added, and a solvent-insoluble residue formed was collected by filtration using a membrane (ADVANTEC H020A047A). It was dried *in vacuo* to obtain poly(**1a-2**) as a yellow solid (22.7 mg) in 30% yield. ^1H NMR (400 MHz, DMSO- d_6): δ 7.50–7.10 (br, 16*n*H), 5.25–5.05 (br, 4*n*H), 3.18–2.82 (br, 4*n*H), 1.50–1.23 (br, 8*n*H) ppm. Unreacted monomer **1a** was also confirmed. IR (KBr): 3410, 3070, 2930, 2110, 1718, 1658, 1621, 1592, 1558, 1486 cm^{-1} . Poly(**1b-2**): 60% yield. ^1H NMR (400 MHz, DMSO- d_6): δ 9.45–9.07 (br, 2*n*H), 8.50–8.25 (br, 2*n*H), 7.80–7.05 (br, 10*n*H), 5.28–5.11 (br, 4*n*H), 3.17–2.91 (br, 4*n*H), 1.41–1.25 (br, 26*n*H) ppm. IR (KBr): 3347, 3029, 2953, 2863, 2114, 1724, 1622, 1511, 1463, 1108 cm^{-1} .

Synthesis of Pt-containing segmented PUs

Segmented PUs were synthesized according to the literature procedure [54]. Typical procedure is as follows. Compound **1b** (14.5 mg, 0.02 mmol) and PTHF (1.96 g, 0.98 mmol) were dissolved in THF (10 mL) under Ar. Then, **2** (0.33 mL, 2.00 mmol) and DBTDL (50 μL , 0.084 mmol) were added, and the resulting mixture was stirred at 60 °C for 3 h. Then, BDO (0.090 mL, 1.00 mmol)

was added to the reaction mixture, and stirred at 60 °C for further 24 h. The reaction mixture was poured into a large amount of MeOH to precipitate a polymer. It was filtrated using a membrane (ADVANTEC H020A047A) and dried *in vacuo* to obtain **SPU_{1b_1.0}** quantitatively. ¹H NMR (400 MHz, CDCl₃): δ 5.19–5.10 (br), 4.90–4.65 (br), 4.20–3.92 (br), 3.51–3.30 (br), 3.20–3.05 (br), 2.90–2.80 (br), 2.41–2.28 (br), 2.20–2.10 (br), 2.05–1.90 (br), 1.82–1.12 (br) ppm. IR (KBr) = 3410, 3070, 2930, 2110, 1718, 1658, 1621, 1592, 1558, 1486 cm⁻¹. **SPU_{1b_2.0}**: 48% yield. ¹H NMR (400 MHz, CDCl₃): δ 4.88–4.55 (br), 4.20–4.01 (br), 3.51–3.35 (br), 3.18–3.05 (br), 2.41–1.90 (br), 1.82–1.23 (br) ppm. IR (KBr) = 3320, 2938, 2854, 2863, 2114, 1718, 1684, 1622, 1105 cm⁻¹.

Computation

Density-functional theory (DFT) calculations were performed with Gaussian 16 [55] using ωB97X-D functional in conjunction with 6-31G* basis set, running on the supercomputer system, Academic Center for Computing and Media Studies, Kyoto University.

Film preparation

A PU sample was dissolved in THF (*c* = 43 mg/mL), and the resulting solution was poured into a Teflon petri dish (Φ = 80 mm) slowly, followed by drying in a fume hood for 24 h to give a self-standing yellowish film.

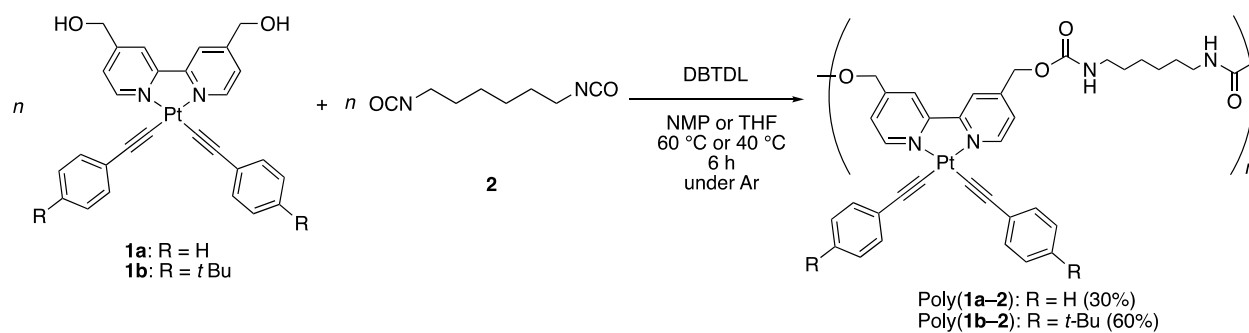
RESULTS AND DISCUSSION

Synthesis of Pt-containing PUs

Hydroxy-tethered Pt(II) complexes **1a** and **1b** were prepared according to Scheme S1. Their chemical structures were confirmed by $^1\text{H}/^{13}\text{C}$ NMR (Figs. 1 and S1–S5), IR absorption (Fig. 2) spectroscopic and high-resolution mass spectrometric analyses. Monomer **1b** was synthesized expecting enhancement of solubility of formed PUs, because **1a** was only soluble in DMSO, DMF and NMP. As expected, **1b** was soluble in CHCl_3 and THF in addition to these solvents. The polyaddition of **1a** and **1b** with **2** was carried out in the presence of a small portion of DBTDL as a catalyst to obtain poly(**1a-2**) and poly(**1b-2**), respectively according to Scheme 1. The polyaddition of **1a** with **2** was conducted in NMP at 60 °C, while that of **1b** with **2** was done in THF at 40 °C considering the solubilities of **1a** and **1b**. The low yield (30%) of poly(**1a-2**) was mainly due to technical loss caused by the low solubility of **1a**. Figs. 1 and S6 show the ^1H NMR spectra of **1a**, **1b**, and poly(**1a-2**), poly(**1b-2**), both in which the benzylic proton peak (H_a) was clearly shifted downfield after polyaddition. However, the contamination of unreacted monomer **1a** was also confirmed in poly(**1a-2**) likely due to the difficult monomer separation from the formed polymer *via* precipitation using MeOH as a poor solvent. The SEC trace (eluent: DMF with 10 mM LiBr) of poly(**1a-2**) also indicated the contamination of **1a** judging from the bimodal peak (Fig. S7a). The first fraction is assignable to poly(**1a-2**), whose M_w and D were estimated to be

16,100 and 1.7 calibrated by polystyrene standards (Table S1), whereas the second fraction is assignable to **1a**. The integration ratio of the first and second fractions was 25/75. On the other hand, a unimodal peak was observed in the SEC of poly(**1b-2**) at a molecular weight region higher than the peak of **1b**, indicating the successful removal of monomer **1b** (Fig. S7b). The M_w and \mathcal{D} of poly(**1b-2**) were estimated to be 18,000 and 2.75. Fig. 2 displays the IR absorption spectra of poly(**1a-2**) and poly(**1b-2**), together with those of **1a** and **1b**. A characteristic peak of Pt-acetylide was observed at 2110 cm^{-1} in the spectra of all the samples, indicating that this bond was intact during the polyaddition and also purification process. Besides, a urethane carbonyl absorption peak was observed at 1720 cm^{-1} in the spectra of poly(**1a-2**) and poly(**1b-2**). The peak intensity of poly(**1b-2**) was larger than that of poly(**1a-2**).

Scheme 1 Synthesis of poly(**1a-2**) and poly(**1b-2**)



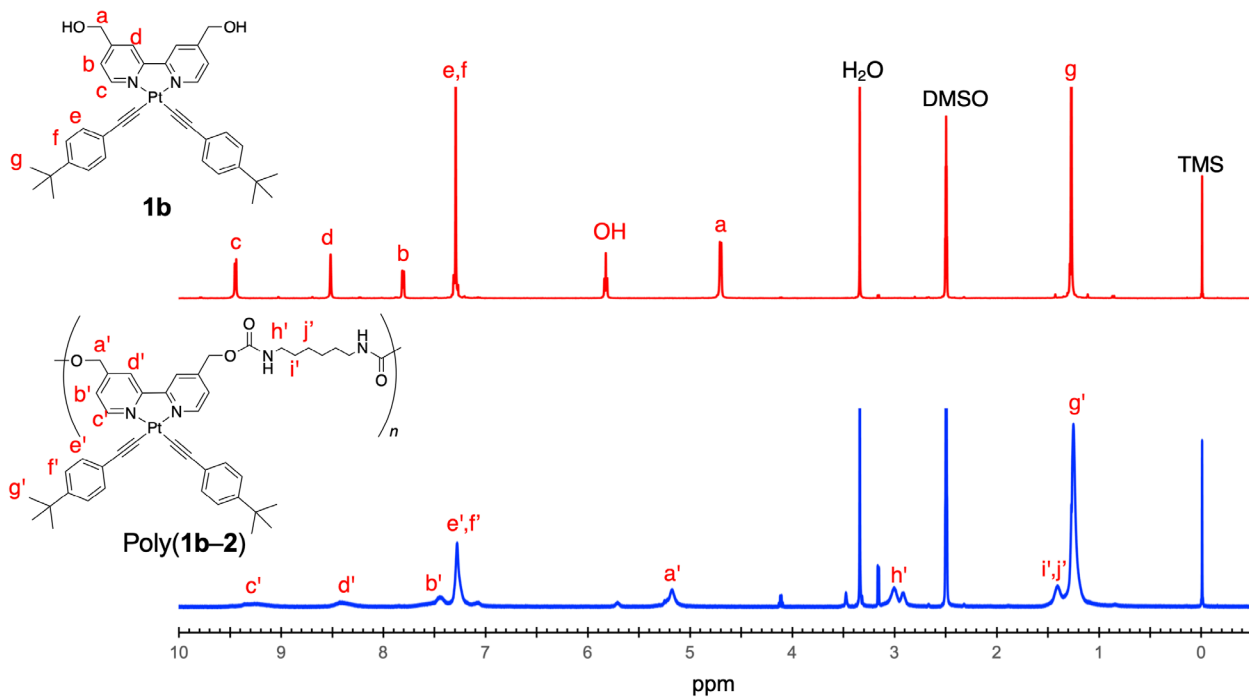


Fig. 1 ^1H NMR spectra of **1b** and **poly(1b-2)** measured in $\text{DMSO-}d_6$ (400 MHz).

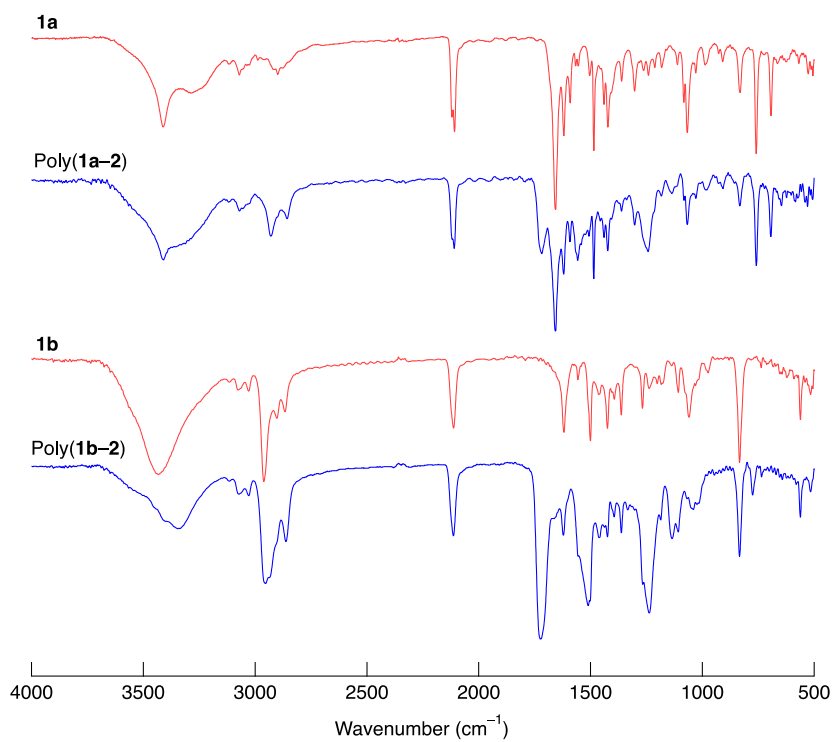


Fig. 2 IR absorption spectra of **1a**, **poly(1a-2)**, **1b** and **poly(1b-2)** (KBr method).

Solution state UV–vis absorption and photoluminescence properties of **1b and poly(**1b–2**)**

The UV–vis absorption and photoluminescence spectra of **1b** and poly(**1b–2**) were measured in DMF ($c = 0.01$ mM). The spectra of poly(**1a–2**) were not measured because of the presence of residual monomer **1a** and poor solubility in common organic solvents. Both **1b** and poly(**1b–2**) showed similar UV–vis absorption peaks as shown in Fig. 3. The peak around 300 nm is assignable to π - π^* transition of the aromatic rings, whereas the peak around 420 nm is metal–ligand and ligand–ligand charge transfer (MLCT and LLCT) transitions. The peaks of poly(**1b–2**) were slightly red-shifted compared to **1b**. To gain knowledge about these transitions, DFT calculations were conducted. The geometries of **1b** and **1b'**, a model compound of poly(**1b–2**) (Fig. S8) were optimized with ω B97X-D functionals, and their UV–vis absorption spectra were simulated by the time-dependent DFT (TD-DFT) method (Figs. S9 and S10). It was confirmed that the peak around 420 nm is MLCT and LLCT transitions, which are mainly assignable to the electronic transitions of HOMO \rightarrow LUMO, HOMO–1 \rightarrow LUMO, HOMO–2 \rightarrow LUMO and HOMO–3 \rightarrow LUMO (Tables S2 and S3). Moreover, the simulated peak top around 400 nm of **1b'** was red-shifted by 30 nm from that of **1b** (Fig. S11), coinciding with the observed results (Fig. 3). The urethane bonds connected to the bipyridine ligand seem to narrow the band gaps inductively, although they do not contribute largely to the delocalization of HOMO and LUMO as shown in Figs. S12 and S13. It is difficult to assign the absorption around 300 nm clearly because of many transitions that contribute

to this absorption. Meanwhile, both **1b** and poly(**1b-2**) showed weak photoluminescence in DMF around 610 nm ($\lambda_{\text{ex}} = 405$ nm) with quantum yields of 1.0 and 0.3%, respectively (Fig. S14). No clear photoluminescence was recognized in the solution state.

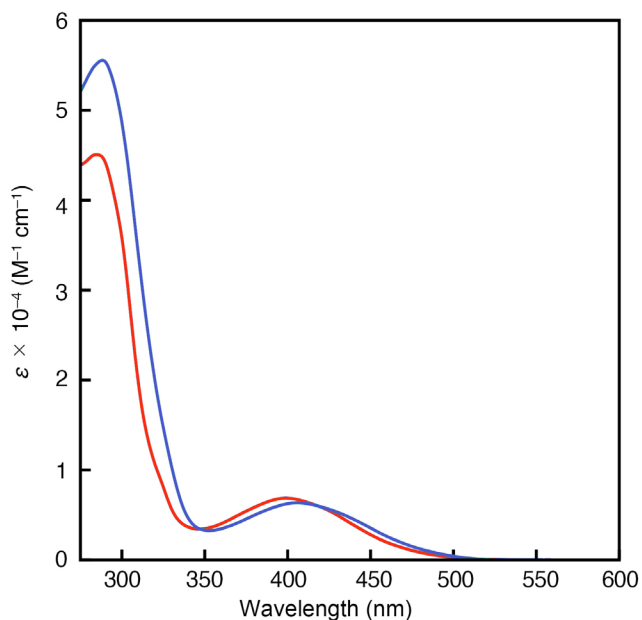


Fig. 3 UV-vis absorption spectra of **1b** (red) and poly(**1b-2**) (blue) measured in DMF ($c = 0.01$ mM).

Mechano(fluoro)chromism of **1b** and poly(**1b-2**)

The mechano(fluoro)chromism of **1b** and poly(**1b-2**) was evaluated by grinding the solid samples in a mortar. Fig. 4 displays the appearance of **1b** and poly(**1b-2**) under ambient and UV-lights ($\lambda_{\text{max}} = 365$ nm). The colors were slightly changed by grinding under ambient light (Fig. 4 a, c). This

color change was also evaluated by UV-vis diffuse reflectance spectroscopy. The reflectance band of **1b** was red-shifted around 30 nm after grinding, whereas no significant change was observed for poly(**1b-2**) (Fig. S15). More obviously, the photoluminescent color of **1b** was changed from yellow to orange (Fig. 4 b), whereas that of poly(**1b-2**) was changed from orange to brown (Fig. 4 d) upon grinding. Further, the fluorescent color changes of **1b** and poly(**1b-2**) were plotted in Commission Internationale de l'Éclairage (CIE) coordinates to determine the photoluminescent color change upon grinding quantitatively (Fig. S16). The difference of the color changes may be caused by the difference of alignment of Pt complex moieties. A series of Pt-bipyridine bis(acetylide) complexes are reported to exhibit appearance and luminescence color changes upon grinding because the distances between Pt-complexes become close [26,56,57]. The similar rearrangement of Pt complex moieties of **1b** and poly(**1b-2**) seems to take place judging from their color changes. The degree of photoluminescent color change of poly(**1b-2**) (Fig. 4 d) was small compared to that of **1b** (Fig. 4 b) after grinding. This result suggests that the Pt-complex moieties of poly(**1b-2**) are closely packed compared to those of **1b** due to intramolecular hydrogen-bonding between the urethane groups. Meanwhile, the chemical structures of **1b** and poly(**1b-2**) after grinding were characterized by ¹H NMR spectroscopic measurements. There was no significant difference before and after grinding, indicating that the chemical structures remained intact after grinding (Figs. S17 and 18). Moreover, the ground samples were dissolved in CHCl₃, and the

obtained solutions were evaporated to check the reversibility of mechano(fluoro)chromism. As results, **1b** and poly(**1b-2**) almost recovered the original appearance and the fluorescent color (Fig. S19).

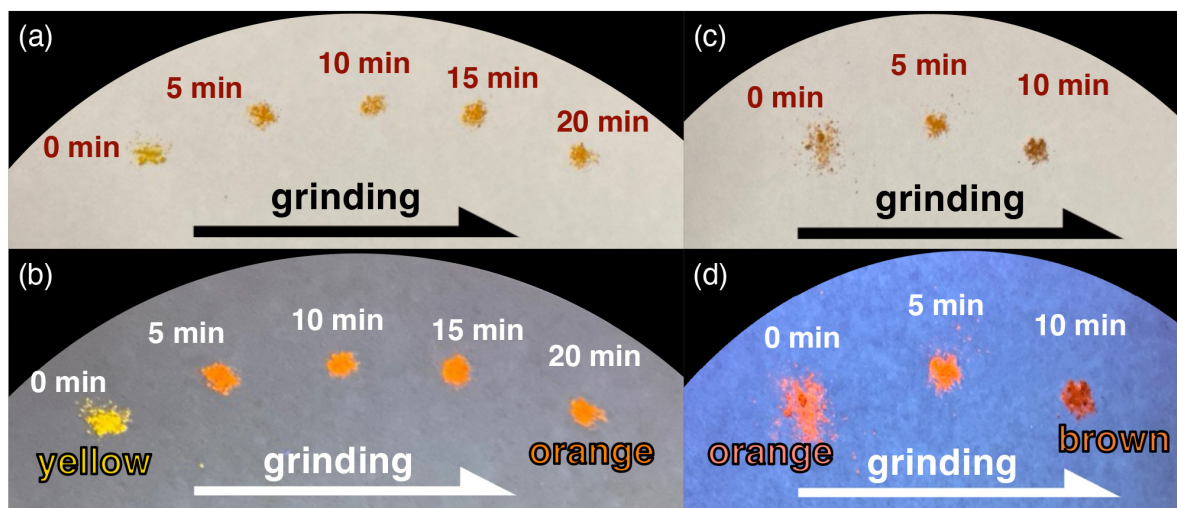


Fig. 4 Photographs of **1b** and poly(**1b-2**) under ambient light (a: **1b** and c: poly(**1b-2**)) and UV-light ($\lambda_{\max} = 365 \text{ nm}$) (b: **1b** and d: poly(**1b-2**)) upon grinding.

Synthesis and characterization of Pt-containing segmented PUs

Although poly(**1b-2**) exhibited distinguishable photoluminescent color changes upon mechanical stress, it was difficult to prepare a self-standing film likely due to its relatively low molecular weights. To obtain PUs with higher molecular weights showing good mechanical properties, poly(**1b-2**)-based segmented PUs, **SPU**_{1b-2_1.0} and **SPU**_{1b-2_2.0} were synthesized according to Scheme 2. The so-called “prepolymer method” was employed using PTHF ($M_n = 2,000$), **2** and

BDO as polymeric diol, diisocyanate and chain extender, respectively, wherein the feed ratios of **1b** were set at 1.0 and 2.0 mol% for **SPU_{1b-2_1.0}** and **SPU_{1b-2_2.0}**, respectively. Further details of feed ratios of the reagents are summarized in Table S4, As expected, both **SPU_{1b-2_1.0}** and **SPU_{1b-2_2.0}** were easily soluble in common organic solvents, and showed higher molecular weights ($M_w = 105,900$ and $43,000$, Table 1) compared to poly(**1b-2**) ($M_w = 18,000$). Hydrogen-bonded N-H and C=O peaks were observed around 3320 and 1705 cm^{-1} in the IR spectra [58,59] together with a weak Pt-acetylide peak around 2100 cm^{-1} (Figs. S20 and S21). Note that the intensity of the latter peak was very weak as the feed ratio of **1b** became small. The UV-vis absorption spectra of **SPU_{1b-2_1.0}** and **SPU_{1b-2_2.0}** were also measured to reveal that the Pt(II) complex moieties were successfully incorporated into the PU backbone judging from the characteristic peaks around 280 and 420 nm (Fig. S22). The absorption intensities of **SPU_{1b-2_2.0}** were larger than those of **SPU_{1b-2_1.0}** as predicted from their incorporated ratios of **1b**. Generally, segmented PUs form microphase separated structures originating from the immiscibility between the crystallized hard segment and soft segment, which largely affect their thermal and mechanical properties [60]. **SPU_{1b-2_1.0}** exhibited a broad SAXS peak as shown in Fig. S23. The domain spacing ($d = 2\pi/q = \lambda/2\sin\theta$, where q is scattering vector, θ is half the scattering angle and λ is the X-ray wavelength) was determined to be approximately 16 nm , which was calculated by using the q value at the peak top of SAXS profile. This value is assignable to the distance between the hard segments of SPUs, and reasonable

compared to the reported ones [54,61,62].

Scheme 2 Synthesis of SPU_{1b-2_1.0} and SPU_{1b-2_2.0}

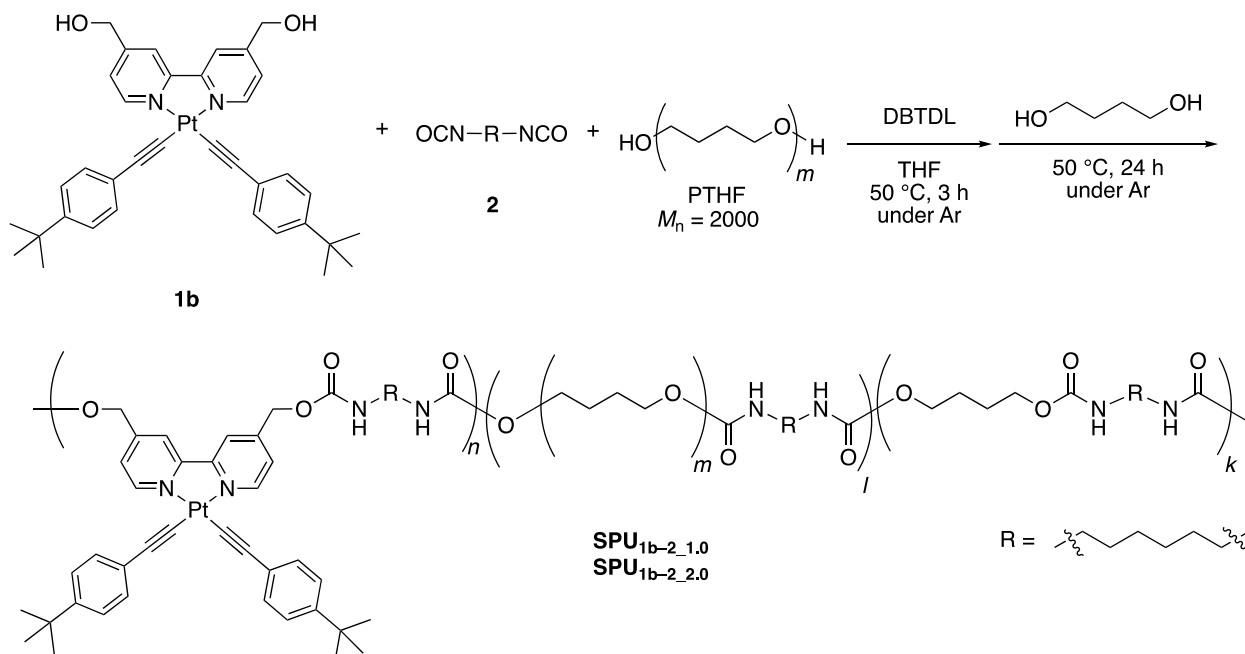


Table 1 Yields and SEC data of SPU_{1b_1.0} and SPU_{1b_2.0}

Polymer	Yield ^a (%)	M_p^b	M_w^b	D^b
SPU _{1b-2_1.0}	quant.	79,900	105,900	2.17
SPU _{1b-2_2.0}	48	39,000	43,000	1.62

^aMeOH-insoluble part.

^bDetected by SEC eluted with THF calibrated by polystyrene standards.

Mechanical properties and mechano(fluoro)chromism of Pt-containing segmented PUs

The mechanical properties of SPU_{1b-2_1.0} and SPU_{1b-2_2.0} were evaluated by tensile tests. Fig. 5

shows the representative stress–strain curves of SPU_{1b-2_1.0} and SPU_{1b-2_2.0} at an elongation rate of

50 mm/min. The breaking strengths of **SPU_{1b-2_1.0}** and **SPU_{1b-2_2.0}** were around 20 MPa. On the other hand, the breaking strain of **SPU_{1b-2_1.0}** was 1.3 times larger than that of **SPU_{1b-2_2.0}**. Thus, the total toughness of **SPU_{1b-2_1.0}** (150 MJ/m³) was larger than that of **SPU_{1b-2_2.0}** (135 MJ/m³), likely reflecting their molecular weights ($M_w = 105,900$ and 43,000). To elucidate their mechano(fluoro)chromism, **SPU_{1b-2_1.0}** was ground in a mortar. **SPU_{1b-2_1.0}** was orangish under ambient light, while significantly luminesced yellowish under UV-light. Upon grinding this elastic sample, their colors did not change significantly (Fig. S24) both under ambient and UV-lights. The tensile tests of the samples were also performed under UV-light to check their photoluminescent color change upon elongation (Fig. S25). However, no clear color change was observed by naked eyes upon elongation of **SPU_{1b-2_1.0}** and **SPU_{1b-2_2.0}** specimen. The high mobility of main chains of the elastic PUs possibly suppressed the reorientation of the Pt(II) complex moieties, resulting in no mechano(fluoro)chromism.

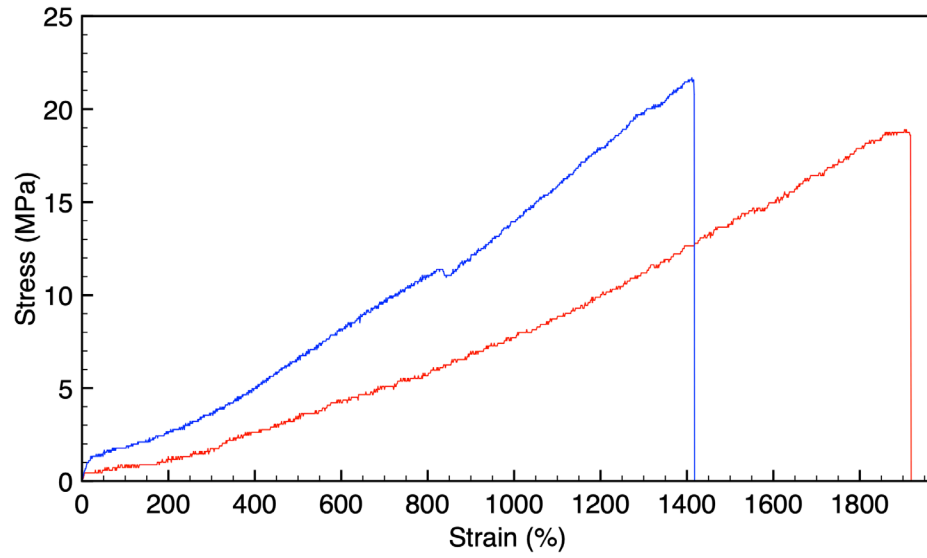


Fig. 5 Representative stress–strain curves of SPU_{1b-2_1.0} (red line) and SPU_{1b-2_2.0} (blue line). Elongation rate: 50 mm/min.

Conclusions

Hydroxy-tethered Pt(II) complexes, **1a** and **1b** were newly synthesized and employed as diol monomers for PU synthesis. By the polyaddition with isocyanate **2**, poly(**1a-2**) was not obtained efficiently due to the poor solubility of **1a**, while poly(**1b-2**) with a moderate molecular weight was successfully obtained, which was well soluble in common organic solvents including CHCl₃ and THF. The photoluminescent color changes of **1b** and poly(**1b-2**) were observed upon grinding at the solid state. Poly(**1b-2**)-based segmented PUs, SPU_{1b-2_1.0} and SPU_{1b-2_2.0} containing Pt(II) complex moieties in the main chain were also synthesized. SPU_{1b-2_1.0} and SPU_{1b-2_2.0} exhibited good mechanical properties, but no clear mechano(fluoro)chromism. It is desirable to optimize the molecular structures and polymerization conditions for controlling the location of Pt complex and the domain balance of hard and soft segments in order to develop useful Pt-containing elastic materials that show both good mechanical properties and mechanoc(fluoro)chromism. Further study is ongoing and will be reported elsewhere in the future.

Supplementary information

¹H and ¹³C NMR spectra of monomers and polymers (Figs. S1–S5); ¹H NMR spectra of **1a** and poly(**1a-2**) (Fig. S6); SEC profiles (Fig. S7); polymerization results (Table S1); chemical structures of **1b** and **1b'** (Fig. S8); simulated UV–vis absorption spectra (Figs. S9–S11); results of TD-DFT

calculations (Tables S2 and S3); shapes of representative molecular orbitals (Figs. S12 and S13); photoluminescence spectra (Fig. S14); UV–vis diffuse reflectance spectra (Fig. S15); CIE plots (Fig. S16); ^1H NMR spectra of **1b** and poly(**1b–2**) before and after grinding (Figs. S17 and S18); photographs of **1b** and poly(**1b–2**) after evaporating CHCl_3 of ground samples (Fig. S19); reaction conditions of **SPU**_{1b–2_1.0} and **SPU**_{1b–2_2.0} (Table S4); IR spectra of **SPU**_{1b–2_1.0} and **SPU**_{1b–2_2.0} (Figs. S20 and S21); UV–vis absorption spectra of **SPU**_{1b–2_1.0} and **SPU**_{1b–2_2.0} (Fig. S22); SAXS profile of **SPU**_{1b–2_1.0} (Fig. S23); mechano(fluoro)chromism of **SPU**_{1b–2_1.0} (Figs. S24 and S25).

Conflict of interest

The authors declare no competing interest.

Acknowledgements

This research was financially supported by JSPS KAKENHI Grant Number JP21K05203, the Kansai University Fund for Supporting Young Scholars, 2021. The synchrotron radiation experiments were performed at beamline BL19B2 of SPring-8 with the approval of the Japan Synchrotron Radiation Research Institute (JASRI) (Proposal 2022B1752). This research used computational resources under Collaborative Research Program for Young•Women Scientists provided by Academic Center for Computing and Media Studies, Kyoto University. The authors

thank Prof. Takashi Miyata, Prof. Akifumi Kawamura and Ms. Chika Hajime (Kansai University)

for letting them use a tensile testing machine.

References

1. Imato K, Otsuka H. Reorganizable and stimuli-responsive polymers based on dynamic carbon–carbon linkages in diarylbibenzofuranones. *Polymer*. 2018;137:395-413.
2. Calvino C, Neumann L, Weder C, Schrettl S. Approaches to polymeric mechanochromic materials. *J Polym Sci Part A: Polym Chem*. 2017;55:640-52.
3. Herbert KM, Schrettl S, Rowan SJ, Weder C. 50th Anniversary Perspective: Solid-State Multistimuli, Multiresponsive Polymeric Materials. *Macromolecules*. 2017;50:8845-70.
4. Sagara Y, Yamane S, Mitani M, Weder C, Kato T. Mechanoresponsive Luminescent Molecular Assemblies: An Emerging Class of Materials. *Adv Mater*. 2016;28:1073-95.
5. Ciardelli F, Ruggeri G, Pucci A. Dye-containing polymers: methods for preparation of mechanochromic materials. *Chem Soc Rev*. 2013;42:857-70.
6. Lee CK, Davis DA, White SR, Moore JS, Sottos NR, Braun PV. Force-Induced Redistribution of a Chemical Equilibrium. *J Am Chem Soc*. 2010;132:16107-11.
7. Davis DA, Hamilton A, Yang J, Cremer LD, Van Gough D, Potisek SL, Ong MT, Braun PV, Martínez TJ, White SR, Moore JS, Sottos NR. Force-induced activation of covalent bonds in mechanoresponsive polymeric materials. *Nature*. 2009;459:68-72.
8. Lu Y, Aoki D, Sawada J, Kosuge T, Sogawa H, Otsuka H, Takata T. Visualization of the slide-ring effect: a study on movable cross-linking points using mechanochromism. *Chem Commun*. 2020;56:3361-64.
9. Ishizuki K, Oka H, Aoki D, Goseki R, Otsuka H. Mechanochromic Polymers That Turn Green Upon the Dissociation of Diarylbibenzothiophenonyl: The Missing Piece toward Rainbow Mechanochromism. *Chem Eur J*. 2018;24:3170-73.
10. Imato K, Kanehara T, Nojima S, Ohishi T, Higaki Y, Takahara A, Otsuka H. Repeatable mechanochemical activation of dynamic covalent bonds in thermoplastic elastomers. *Chem*

- Commun. 2016;52:10482-85.
11. Oka H, Imato K, Sato T, Ohishi T, Goseki R, Otsuka H. Enhancing Mechanochemical Activation in the Bulk State by Designing Polymer Architectures. *ACS Macro Lett.* 2016;5:1124-27.
 12. Imato K, Irie A, Kosuge T, Ohishi T, Nishihara M, Takahara A, Otsuka H. Mechanophores with a Reversible Radical System and Freezing-Induced Mechanochemistry in Polymer Solutions and Gels. *Angew Chem Int Ed.* 2015;54:6168-72.
 13. Sagara Y, Traeger H, Li J, Okado Y, Schrettl S, Tamaoki N, Weder C. Mechanically Responsive Luminescent Polymers Based on Supramolecular Cyclophane Mechanophores. *J Am Chem Soc.* 2021;143:5519-25.
 14. Traeger H, Sagara Y, Kiebala DJ, Schrettl S, Weder C. Folded Perylene Diimide Loops as Mechanoresponsive Motifs. *Angew Chem Int Ed.* 2021;60:16191-99.
 15. Xue P, Ding J, Wang P, Lu R. Recent progress in the mechanochromism of phosphorescent organic molecules and metal complexes. *J Mater Chem C.* 2016;4:6688-706.
 16. Wenger OS. Vapochromism in Organometallic and Coordination Complexes: Chemical Sensors for Volatile Organic Compounds. *Chem Rev.* 2013;113:3686-733.
 17. Zhang X, Chi Z, Zhang Y, Liu S, Xu J. Recent advances in mechanochromic luminescent metal complexes. *J Mater Chem C.* 2013;1:3376-90.
 18. Ito H, Muromoto M, Kurenuma S, Ishizaka S, Kitamura N, Sato H, Seki T. Mechanical stimulation and solid seeding trigger single-crystal-to-single-crystal molecular domino transformations. *Nature Commun.* 2013;4:2009.
 19. Seki T, Ozaki T, Okura T, Asakura K, Sakon A, Uekusa H, Ito H. Interconvertible multiple photoluminescence color of a gold(i) isocyanide complex in the solid state: solvent-induced blue-shifted and mechano-responsive red-shifted photoluminescence. *Chem Sci.* 2015;6:2187-95.

20. Ito H, Saito T, Oshima N, Kitamura N, Ishizaka S, Hinatsu Y, Wakeshima M, Kato M, Tsuge K, Sawamura M. Reversible Mechanochromic Luminescence of [(C₆F₅Au)₂(μ-1,4-Diisocyanobenzene)]. *J Am Chem Soc.* 2008;130:10044-45.
21. Lien C-Y, Hsu Y-F, Liu Y-H, Peng S-M, Shinmyozu T, Yang J-S. Steric Engineering of Cyclometalated Pt(II) Complexes toward High-Contrast Monomer–Excimer-Based Mechanochromic and Vapochromic Luminescence. *Inorganic Chem.* 2020;59:11584-94.
22. Norton AE, Abdolmaleki MK, Liang J, Sharma M, Golsby R, Zoller A, Krause JA, Connick WB, Chatterjee S. Phase transformation induced mechanochromism in a platinum salt: a tale of two polymorphs. *Chem Commun.* 2020;56:10175-78.
23. Choi SJ, Kuwabara J, Nishimura Y, Arai T, Kanbara T. Two-step Changes in Luminescence Color of Pt(II) Complex Bearing an Amide Moiety by Mechano- and Vapochromism. *Chem Lett.* 2011;41:65-67.
24. Nishiuchi Y, Takayama A, Suzuki T, Shinozaki K. A Polymorphic Platinum(II) Complex: Yellow, Red, and Green Polymorphs and X-ray Crystallography of [Pt(fdpb)Cl] [Hfdpb = 1,3-Bis(5-trifluoromethyl-2-pyridyl)benzene]. *Eur J Inorg Chem.* 2011;2011:1815-23.
25. Abe T, Itakura T, Ikeda N, Shinozaki K. Luminescence color change of a platinum(II) complex solid upon mechanical grinding. *Dalton Trans.* 2009;711-15.
26. Kang J, Zhang X, Zhou H, Gai X, Jia T, Xu L, Zhang J, Li Y, Ni J. 1-D “Platinum Wire” Stacking Structure Built of Platinum(II) Diimine Bis(σ-acetylide) Units with Luminescence in the NIR Region. *Inorganic Chem.* 2016;55:10208-17.
27. Ni J, Wang Y-G, Wang H-H, Pan Y-Z, Xu L, Zhao Y-Q, Liu X-Y, Zhang J-J. Reversible Dual-Stimulus-Responsive Luminescence and Color Switch of a Platinum Complex with 4-[(2-Trimethylsilyl)ethynyl]-2,2'-bipyridine. *Eur J Inorg Chem.* 2014;2014:986-93.
28. Zhang X, Wang J-Y, Ni J, Zhang L-Y, Chen Z-N. Vapochromic and Mechanochromic Phosphorescence Materials Based on a Platinum(II) Complex with 4-Trifluoromethylphenylacetylide. *Inorganic Chem.* 2012;51:5569-79.

29. Ni J, Zhang X, Wu Y-H, Zhang L-Y, Chen Z-N. Vapor- and Mechanical-Grinding-Triggered Color and Luminescence Switches for Bis(σ -fluorophenylacetylide) Platinum(II) Complexes. *Chem Eur J.* 2011;17:1171-83.
30. Geng H, Luo K, Zou G, Wang H, Ni H, Yu W, Li Q, Wang Y. New phosphorescent platinum(ii) complexes: lamellar mesophase and mechanochromism. *New J Chem.* 2016;40:10371-77.
31. Ohno K, Yamaguchi S, Nagasawa A, Fujihara T. Mechanochromism in the luminescence of novel cyclometalated platinum(ii) complexes with α -aminocarboxylates. *Dalton Trans.* 2016;45:5492-503.
32. Krikorian M, Liu S, Swager TM. Columnar Liquid Crystallinity and Mechanochromism in Cationic Platinum(II) Complexes. *J Am Chem Soc.* 2014;136:2952-55.
33. Zhang D, Wu L-Z, Yang Q-Z, Li X-H, Zhang L-P, Tung C-H. Versatile Photosensitization System for 1O₂-Mediated Oxidation of Alkenes Based on Nafion-Supported Platinum(II) Terpyridyl Acetylide Complex. *Organic Lett.* 2003;5:3221-24.
34. Li X-H, Wu LZ, Zhang LP, Tung C-H, Che C-M. Luminescence and photocatalytic properties of a platinum(II)-quaterpyridine complex incorporated in Nafion membrane. *Chem Commun.* 2001;2280-81.
35. Liu N, Wang Y, Wang C, He Q, Bu W. Syntheses and Controllable Self-Assembly of Luminescence Platinum(II) Plane-Coil Diblock Copolymers. *Macromolecules.* 2017;50:2825-37.
36. Kumpfer JR, Taylor SD, Connick WB, Rowan SJ. Vapochromic and mechanochromic films from square-planar platinum complexes in polymethacrylates. *J Mater Chem.* 2012;22:14196-204.
37. Aoki R, Horiuchi T, Makino S, Sano N, Imai Y, Sogawa H, Sanda F. Chirality induction in platinum-containing polyaryleneethynyls by exchange from achiral phosphine ligands to P-chiral phosphine ligands. *Polymer.* 2023;265:125576.

38. Ishida T, Sotani T, Sano N, Sogawa H, Sanda F. Control of Higher-Order Structures of Platinum-Containing Conjugated Polymers by Ligand Exchange Reactions: Chirality Transfer from Optically Active Ligands to Optically Inactive Polymers. *Macromolecules*. 2022;55:309-21.
39. Makino S, Horiuchi T, Ishida T, Sano N, Yajima T, Sogawa H, Sanda F. Synthesis of Platinum-Containing Conjugated Polymers Bearing Chiral Phosphine Ligands. Study of Geometries and Intermolecular Interactions Leading to Aggregation. *Organometallics*. 2022;41:1699-709.
40. Marumoto M, Sotani T, Miyagi Y, Yajima T, Sano N, Sanda F. Synthesis of Platinum-Containing Conjugated Polymers Having QuinoxP* and Bipyridine Ligands. Chirality Transfer from the Phosphine Ligand to the Polymer Backbone. *Macromolecules*. 2020;53:2031-38.
41. Sotani T, Yajima T, Sogawa H, Sanda F. Synthesis of Platinum-Containing Conjugated Polymers Bearing Optically Active Amide Groups: A Mechanistic Study of Chiral Aggregation. *Macromolecules*. 2020;53:11077-88.
42. Miyagi Y, Ishida T, Marumoto M, Sano N, Yajima T, Sanda F. Ligand Exchange Reaction for Controlling the Conformation of Platinum-Containing Polymers. *Macromolecules*. 2018;51:815-24.
43. Miyagi Y, Sotani T, Yajima T, Sano N, Sanda F. Effect of phosphine ligand on the optical absorption/emission properties of platinum-containing conjugated polymers. *Polym Chem*. 2018;9:1772-79.
44. Miyagi Y, Shibutani Y, Otaki Y, Sanda F. Synthesis of platinum-containing poly(phenyleneethynylene)s having various chromophores: aggregation and optical properties. *Polym Chem*. 2016;7:1070-78.
45. Otaki Y, Marumoto M, Miyagi Y, Hirao T, Haino T, Sanda F. Synthesis and Properties of Novel Optically Active Platinum-containing Poly(phenyleneethynylene)s. *Chem Lett*. 2016;45:937-39.

46. Miyagi Y, Hirao T, Haino T, Sanda F. Synthesis of optically active conjugated polymers containing platinum in the main chain: Control of the higher-order structures by substituents and solvents. *J Polym Sci Part A: Polym Chem.* 2015;53:2452-61.
47. Inoue Y, Ishida T, Sano N, Yajima T, Sogawa H, Sanda F. Platinum-Mediated Reversible Cross-linking/Decross-linking of Polyacetylenes Substituted with Phosphine Ligands: Catalytic Activity for Hydrosilylation. *Macromolecules.* 2022;55:5711-22.
48. Uchiyama S, Sotani T, Mizokuro T, Sogawa H, Wagener KB, Sanda F. End Functionalization of Polynorbornene with Platinum–Acetylide Complexes Utilizing a Cross-Metathesis Reaction. *Macromolecules.* 2023;56:281-91.
49. Sotani T, Mizokuro T, Yajima T, Sogawa H, Sanda F. Highly photoluminescent poly(norbornene)s carrying platinum–acetylide complex moieties in their side chains: evaluation of oxygen sensing and TTA–UC. *Polym Chem.* 2021;12:4829-37.
50. Menon AV, Madras G, Bose S. The journey of self-healing and shape memory polyurethanes from bench to translational research. *Polym Chem.* 2019;10:4370-88.
51. Delebecq E, Pascault J-P, Boutevin B, Ganachaud F. On the Versatility of Urethane/Urea Bonds: Reversibility, Blocked Isocyanate, and Non-isocyanate Polyurethane. *Chem Rev.* 2013;113:80-118.
52. Chattopadhyay DK, Raju KVS. Structural engineering of polyurethane coatings for high performance applications. *Prog Polym Sci.* 2007;32:352-418.
53. Osaka K, Matsumoto T, Taniguchi Y, Inoue D, Sato M, Sano N. High-throughput and automated SAXS/USAXS experiment for industrial use at BL19B2 in SPring-8. *AIP Conference Proceedings.* 2016;1741:030003.
54. Sawada J, Sogawa H, Marubayashi H, Nojima S, Otsuka H, Nakajima K, Akae Y, Takata T. Segmented polyurethanes containing movable rotaxane units on the main chain: Synthesis, structure, and mechanical properties. *Polymer.* 2020;193:122358.
55. Frisch Me, Trucks G, Schlegel HB, Scuseria G, Robb M, Cheeseman J, Scalmani G, Barone

- V, Petersson G, Nakatsuji H. Gaussian 16.). Gaussian, Inc. Wallingford, CT (2016).
56. Su M-M, Kang J-J, Liu S-Q, Meng C-G, Li Y-Q, Zhang J-J, Ni J. Strategy for Achieving Long-Wavelength Near-Infrared Luminescence of Diimineplatinum(II) Complexes. *Inorganic Chem.* 2021;60:3773-80.
 57. Wong KM-C, Yam VW-W. Self-Assembly of Luminescent Alkynylplatinum(II) Terpyridyl Complexes: Modulation of Photophysical Properties through Aggregation Behavior. *Acc Chem Res.* 2011;44:424-34.
 58. Pattanayak A, Jana SC. Thermoplastic polyurethane nanocomposites of reactive silicate clays: effects of soft segments on properties. *Polymer.* 2005;46:5183-93.
 59. Ning L, De-Ning W, Sheng-Kang Y. Crystallinity and hydrogen bonding of hard segments in segmented poly(urethane urea) copolymers. *Polymer.* 1996;37:3577-83.
 60. Kojio K, Nozaki S, Takahara A, Yamasaki S. Influence of chemical structure of hard segments on physical properties of polyurethane elastomers: a review. *J Polym Res.* 2020;27:140.
 61. Rahmawati R, Nozaki S, Kojio K, Takahara A, Shinohara N, Yamasaki S. Microphase-separated structure and mechanical properties of cycloaliphatic diisocyanate-based thiourethane elastomers. *Polym J.* 2019;51:265-73.
 62. Koberstein JT, Russell TP. Simultaneous SAXS-DSC study of multiple endothermic behavior in polyether-based polyurethane block copolymers. *Macromolecules.* 1986;19:714-20.